Journal of Magnetism and Magnetic Materials 517 (2021) 167236

Contents lists available at ScienceDirect

Journal of Magnetism and Magnetic Materials

journal homepage: www.elsevier.com/locate/jmmm

Research articles

Phase-transition-induced magneto-elastic coupling and negative thermal expansion in (Hf,Ta)$Fe_{1.98}$ Laves phase

Shuai Li[a], Jiancheng Yang[a], Ni Zhao[a], Qiang Wang[b], Xiaomeng Fan[c], Xiaowei Yin[c], Weibin Cui[a,d,*]

[a] Key Laboratory of Electromagnetic Processing of Materials, Northeastern University, Shenyang 110819, China
[b] State Key Laboratory of Rolling and Automation, Northeastern University, Shenyang 110819, China
[c] State Key Laboratory of Solidification Processing, Northwestern Polytechnical University, Xi'an 710072, China
[d] Department of Physics and Chemistry of Materials, School of Material Science and Engineering, Northeastern University, Shenyang 110819, China

ARTICLE INFO

Keywords:
(Hf,Ta)Fe_2 Laves phase
Magneto-elastic coupling
Magnetocaloric effects
Negative thermal expansion
Magnetostriction

ABSTRACT

The effects of Ta substitution on the phase transition have been studied in $Hf_{1-x}Ta_xFe_{1.98}$ (x = 0.125, 0.13, 0.135) alloys with kagome-type lattice. Increased Ta substitution leads into the reduced metamagnetic transition temperature (T_t). The nature of such phase transition is also changed from second-order type to the weak first-order one, suggested by the gradually observed hysteresis. The magnetic entropy change (ΔS) is meanwhile enhanced from 3.04 J kg^{-1} K^{-1} to 3.4 J kg^{-1} K^{-1}. Such enhanced magnetocaloric effects are strongly correlated with the enhanced magneto-elastic effect, which is further confirmed by the maximized saturation magnetostriction ($\lambda^s_{//}$) of ~1700 ppm near the T_t of $Hf_{0.865}Ta_{0.135}Fe_{1.98}$ alloy. The concurrence of maximized ΔS^{max} and $\lambda^s_{//}$ suggests the strong magneto-elastic coupling during phase transition and the high linear co-efficiency of negative thermal expansion can be triggered in Fe-deficient $Hf_{0.865}Ta_{0.135}Fe_{1.98}$ alloy.

1. Introduction

AFe_2 Laves phase compounds, where A can be early transition elements and rare-earth elements, have been a subject of intensive experimental and theoretical investigations. The interesting relationship between the magnetism and the crystal structure has been found. The magnetic ordering is sensitively dependent on the elements at A site. In $MgZn_2$-type hexagonal structure, $ScFe_2$ and $HfFe_2$ phase exhibit the ferromagnetism [1,2]. $TiFe_2$ [3] and $TaFe_2$ [4] show the antiferromagnetism. But $NbFe_2$ phase displays the ground state of spin-density wave [5,6]. As comparison, when rare-earth elements occupy A site, the cubic structure (C15) is formed with interesting magnetism. Particularly, RFe_2 (R = Tb, Dy) phase is well known as magnetostriction materials. Among them, $HfFe_2$ system has attracted lots of attentions in the past decades. Its Curie temperature (T_c) is as high as 600 K [2,7]. By chemical tuning with the other end member with different magnetic ground state, the critical point between ferromagnetic, antiferromagnetic and paramagnetic phases could be realized in recently reported (Hf, Nb)Fe_2 [8] and well-studied (Hf,Ta)Fe_2 systems. When Ta substitution amount, x in $Hf_{1-x}Ta_xFe_2$ alloy, is lower than 0.1, the FM ground state is still preserved. For $0.1 \le x \le 0.3$, the first-order phase transformation is observed with increasing temperature without change in the crystal symmetry but significant change in volume [9,10]. Based on such phase transformation, many investigations on the magnetic properties [11–15], electronic properties [16,17], potential applications in giant magneto-resistance [9,18] have been reported. Due to the interesting magnetic phase transition occurred in $Hf_{1-x}Ta_xFe_2$ ($0.1 \le x \le 0.3$) alloys, the magnetic configuration in FM state and AFM state has been the research topic for a long time and studied by using neutron powder diffraction and Mössbauer spectrum. Dujin et al proposed that all Fe moment carrying 1 μ_B should be aligned within in basal plane in the FM state [9] in contrary to the alignment along c-axis proposed by Nishihara et al. [12–14]. In pseudobinary $Hf_{0.82}Ta_{0.18}Fe_2$ alloy, the alignment within basal plane of Fe moments at FM state is proposed by Mössbauer spectrum [19]. Additionally, during phase transition from FM to AFM, the spin flipping from in-plane to c-axis is deduced by Mössbauer spectrum [19].

But the in-plane triangle kagome-like alignment of Fe moments in the AFM state is proposed by neutron powder diffraction [20]. These results indicate that magnetic structure is still not concluded. Besides, the phase transition is also sensitive to the Fe composition. Herbst et al has studied the effects of Fe-rich and Fe-lean composition on the structure, magnetic and magnetocaloric properties of $(Hf_{0.83}Ta_{0.17})Fe_{2+x}$ alloys. $MgZn_2$-phase can be formed in a wide composition

* Corresponding author at: Key Laboratory of Electromagnetic Processing of Materials, Northeastern University, Shenyang 110819, China.
E-mail address: wbcui2014@outlook.com (W. Cui).

https://doi.org/10.1016/j.jmmm.2020.167236
Received 19 November 2019; Received in revised form 12 July 2020; Accepted 12 July 2020
Available online 18 July 2020
0304-8853/

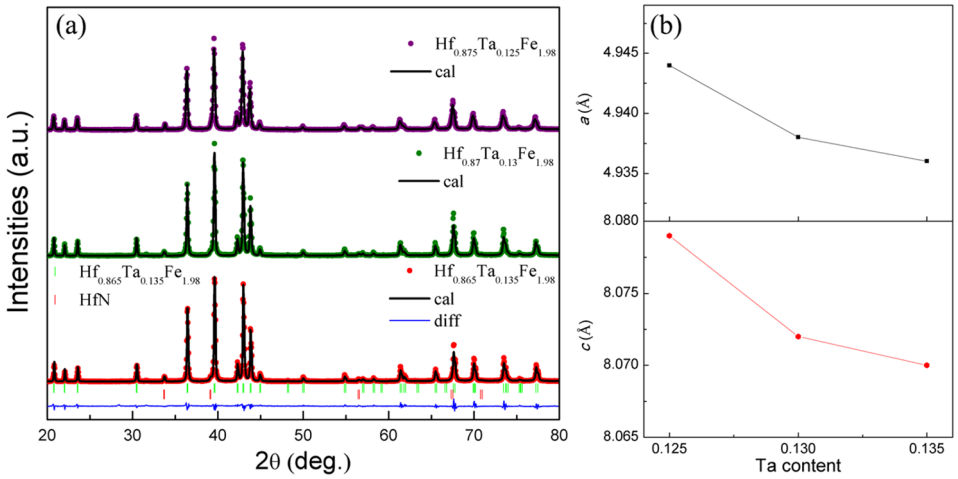

Fig. 1. (a) The refined XRD patterns and (b) the Ta-compositional dependent lattice paramters a and c of $Hf_{1-x}Ta_xFe_{1.98}$ (x = 0.125, 0.13 and 0.135) alloys.

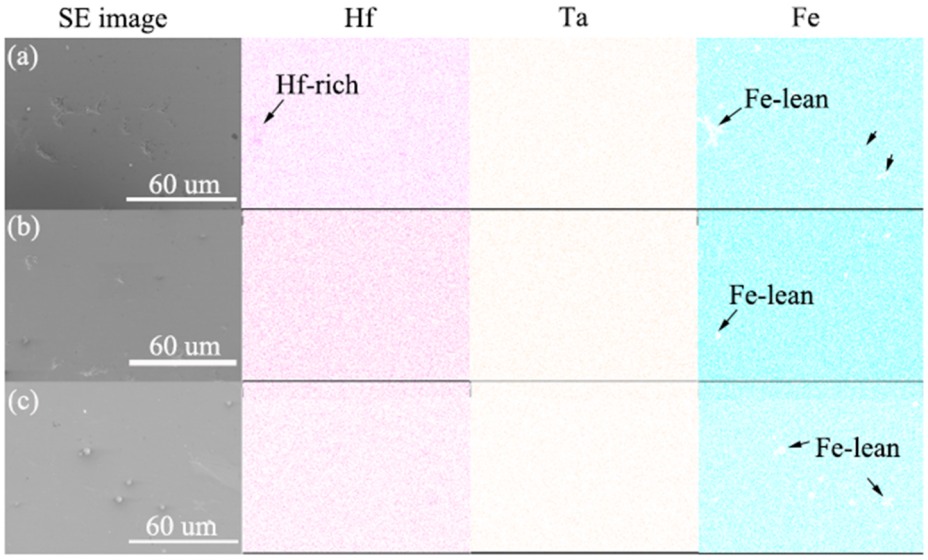

Fig. 2. The SEM images of $Hf_{1-x}Ta_xFe_{1.98}$ (x = (a) 0.125, (b) 0.13 and (c) 0.135) alloys and the corresponding Hf, Ta and Fe elementary distributions.

accompanied with the varied phase transition temperature and magnetic entropy changes [21]. The phase transition can be sharpened by Fe vacancies [22]. The effects of Co substitution for Fe in $Hf_{0.8}Ta_{0.2}Fe_{1.98-x}Co_x$ alloys have also been studied [23]. Recently, Li et al have reported a linear NTE coefficient of −16.3 ppm/K in a wide temperature range of 105 K in a stoichiometric (Hf,Ta)Fe_2 system, due to the first-order nature of phase transition [24]. Therefore, in present work, we started from the Fe-deficient $Hf_{1-x}Ta_xFe_{1.98}$ (x = 0.125,0.13 and 0.135) system, the magnetic phase transition and the corresponding magnetocaloric effects by Ta substitution had been studied. Meanwhile, due to the first-order nature, the magnetostriction near the phase transition temperature was also studied.

2. Experiments

The $Hf_{1-x}Ta_xFe_{1.98}$ (x = 0.125,0.13 and 0.135) alloys used for present investigation was prepared by arc-melting appropriate raw materials with purity higher than 99.99% in the water-cooled copper crucible under a high purity Ar atmosphere. The sample weight loss after arc-melting was less than 1%. In order to make the alloy homogenization, the samples were melt 4 times. The ingots were then annealed at 1073 K for 4 days followed by the furnace cooling. The room-temperature X-ray powder diffraction patterns were taken by using Cu-K_α to examine the phase purity. The microstructure was observed by JOEL JSM-7001F scanning electron miscroscope (SEM). The temperature/field-dependent magnetic properties and linear thermal expansion along the magnetic field direction were measured by Cryogenic physical property measurement systems with max field up to 7 T.

3. Results and discussions

Fig. 1a compares the refined XRD patterns of $Hf_{1-x}Ta_xFe_{1.98}$ (x = 0.125, 0.13 and 0.135) alloys. From the refinement, the main $MgZn_2$-type Laves phase is achieved in all ingots. Besides, the additional impurity phase is detected and determined to be HfN [25]. According to the refinement, the volume ratio of HfN is ranged between 2.51% and 3.08%. The lattice parameters are also calculated and shown in Fig. 1b. Compared with those of $HfFe_2$ phase, the lattice parameter a gradually shrinks within basal plane as well as c along axial direction, which means that the Ta substitution leads into the constrain of hexagonal cell.

The microstructure of $Hf_{1-x}Ta_xFe_{1.98}$ (x = 0.125, 0.13 and 0.135) alloys are carried out by SEM and compared in Fig. 2 along with the Hf, Ta and Fe elementary distributions. In all three alloys, some Fe-lean regions can be observed as marked, corresponding to be Hf-rich. It is consistent with XRD results that there is HfN impurity phase. Besides, it

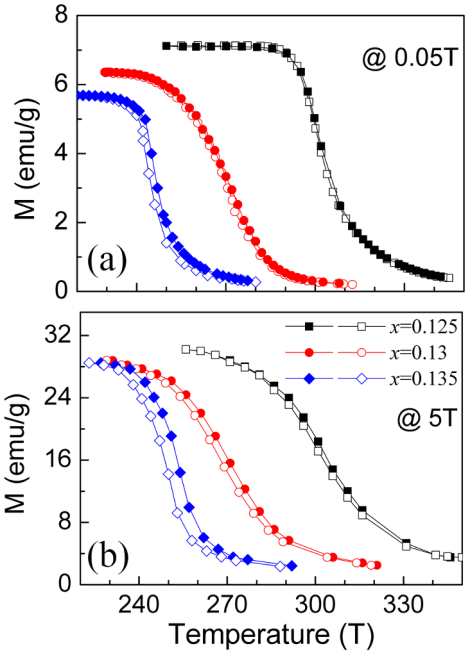

Fig. 3. The thermal magnetization curves of $Hf_{1-x}Ta_xFe_{1.98}$ (x = 0.125, 0.13 and 0.135) alloys measured under (a) 0.05 T and (b) 5 T at the heating (closed symbols) and cooling (open symbols) process.

is seen that there is no observable segregation between Hf and Ta, which is not like the considerable elementary segregation in $(Hf,Ti)Fe_2$ [26] and $(Hf_{0.80}Nb_{0.20})Fe_2$ [8] cases.

Since Ta substitution causes the phase transition, Fig. 3a compares the thermal magnetization curves of $Hf_{1-x}Ta_xFe_{1.98}$ (x = 0.125, 0.13 and 0.135) alloys. During the cooling process, the magnetization gradually increases in $Hf_{0.875}Ta_{0.125}Fe_{1.98}$ alloy, indicating the phase transition gradually from AFM state to FM state, with Curie temperature (T_c) of 303 K. Noting that magnetization of heating process is overlapped with that of cooling process, the good reversibility is observed, indicating the typical second-order nature. However, higher Ta substitution leads into the lowered T_c to ~270 K in $Hf_{0.87}Ta_{0.13}Fe_{1.98}$ alloy and 246 K in $Hf_{0.865}Ta_{0.135}Fe_{1.98}$ alloy. While the thermal hysteresis of ~2 K is observed, indicating the nature of phase transition is changed to the first-order one in $Hf_{0.865}Ta_{0.135}Fe_{1.98}$ alloys. However, above T_c of $Hf_{1-x}Ta_xFe_{1.98}$ (x = 0.125,0.13 and 0.135) alloys, the peak standing for the phase transition from AFM to PM as observed in stoichiometric $Hf_{1-x}Ta_xFe_2$ is not detected. By applying 5 T, the magnetization changes become slowly with temperature (Fig. 3b). The good reversibility is obtained in $Hf_{0.875}Ta_{0.125}Fe_{1.98}$ alloy, confirming the second-order nature. While the thermal hysteresis is widened to 4 K in $Hf_{0.865}Ta_{0.135}Fe_{1.98}$ alloy, which means the typical first-order nature.

To further characterize the phase transition, the isothermal magnetization curves of $Hf_{1-x}Ta_xFe_{1.98}$ (x = 0.125, 0.13 and 0.135) alloys are plotted in Fig. 4a to Fig. 4c as well as the corresponding Arrot plots. In $Hf_{0.875}Ta_{0.125}Fe_{1.98}$ alloy, at low temperature of 285 K, the *S*-shaped magnetization is observed with good reversibility. With increased temperature, the irreversibility of magnetization is observed within 3 T, which is mainly due to the magnetic hysteresis. All these field-increasing and field-decreasing magnetization curves display the similar S-shape as that measured at 285 K. The linear dependence of magnetization versus magnetic field at further increased temperature indicates the completed phase transition to paramagnetic state. In $Hf_{0.87}Ta_{0.13}Fe_{1.98}$ alloy, the M − H curves at low temperature also shows the typical ferromagnetic S-shape. However, at 295 K and 300 K, a linear dependence is observed at low field, followed by the curling at high field, indicating the weak feature of phase transition from PM to FM state. In $Hf_{0.865}Ta_{0.135}Fe_{1.98}$ alloy, between 250 K and 290 K, with increasing field, a weak step-like feature is observed, indicating the weak field-induced phase transition from PM to FM. However, from the field-increasing and field-decreasing processes, small hysteresis is observed. Such field-induced phase transition is obviously of first-order. Since no thermal and magnetic hysteresises are not sufficient to conclude the nature of phase transition, the Arrot plots are also compared in Fig. 4d to Fig. 4f. In $Hf_{0.875}Ta_{0.125}Fe_{1.98}$ alloy, near its T_c, the almost linear dependence of M^2-H/M curves are observed. With increased Ta

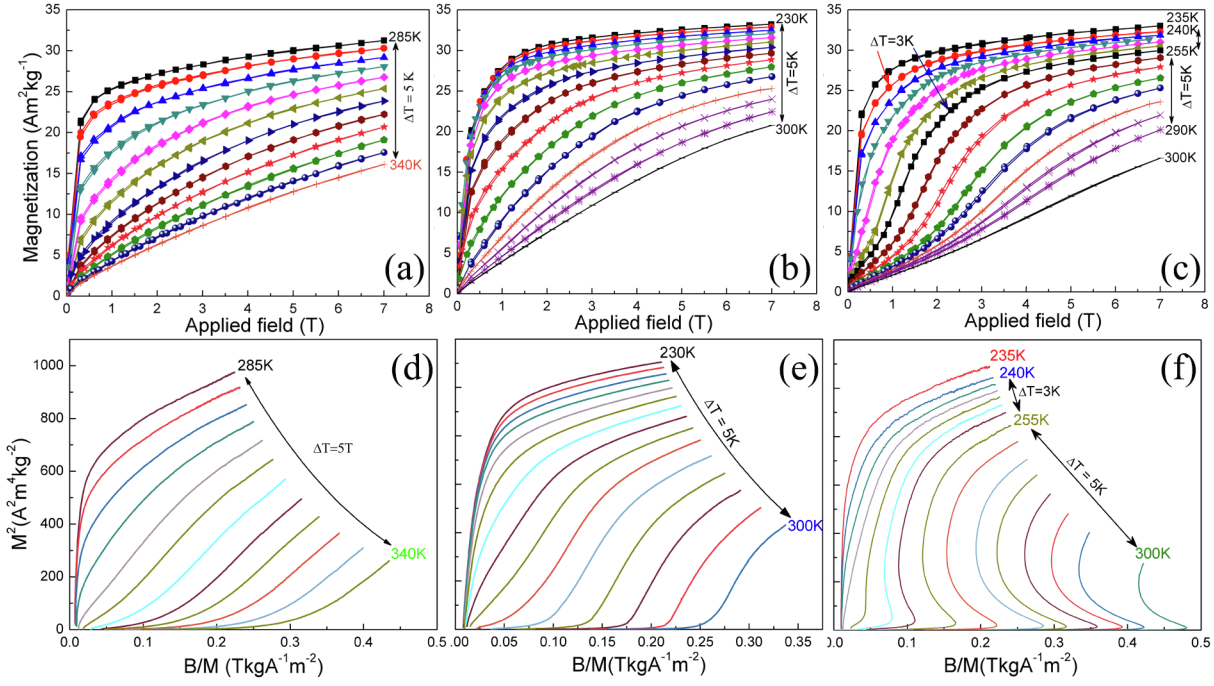

Fig. 4. The temperature-dependent magnetization curves of $Hf_{1-x}Ta_xFe_{1.98}$ (x = (a) 0.125, (b) 0.13 and (c) 0.135) alloys and their corresponding Arrot plots in (d), (e) and (f). The M-μ_0H curves in Fig. 4-c are measured in the increasing/decreasing-field process with observed magnetic hysteresis.

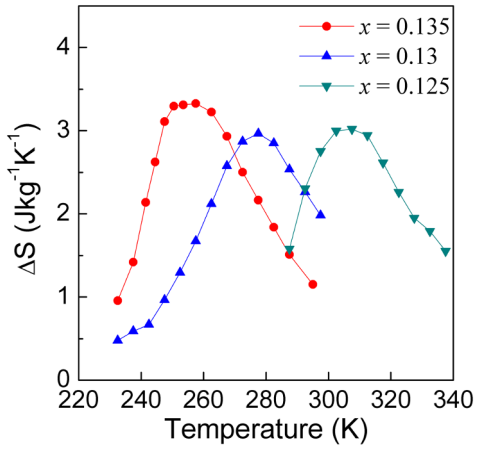

Fig. 5. The temperature dependence of magnetic entropy changes (ΔS) of $Hf_{1-x}Ta_xFe_{1.98}$ (x = 0.125, 0.13 and 0.135) alloys measured under the field change of 7 T.

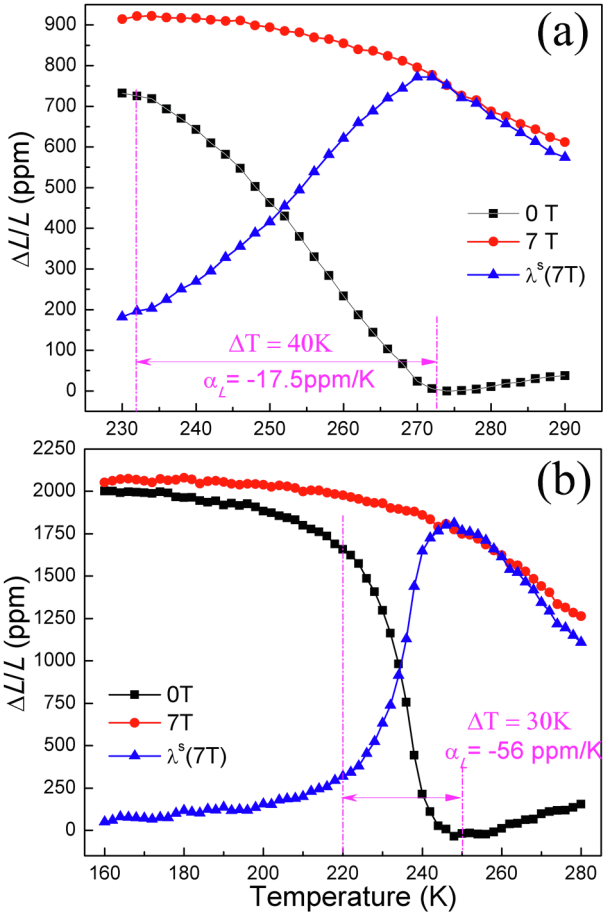

Fig. 6. The temperature-dependent thermal expansion ($\Delta L/L$) measured under 0 T (black squares) and 7 T (red circles) and the saturation magnetostriction measured parallel with the direction of magnetic field (λ^s(7 T)) under 7 T of $Hf_{1-x}Ta_xFe_{1.98}$ (x = (a) 0.13 and (b) 0.135) alloys. (For interpretation of the references to colour in this figure legend, the reader is referred to the web version of this article.)

substitution amount, M^2-H/M curves near T_c becomes gradualled curled, which also confirms the evolved nature of phase transition from the second order in $Hf_{0.875}Ta_{0.125}Fe_{1.98}$ alloy to the weak first-order in $Hf_{0.865}Ta_{0.135}Fe_{1.98}$ alloy. Since impurity phases are observed in all samples by XRD and EDS mapping, such evolution of the order of phase transition is obviously intrinsically caused by the Ta substitution instead of the impurity phase.

Due to the field-induced metamagnetic phase transition, the magnetic entropy changes are calculated by Maxwell relationship and compared in Fig. 5. It is seen that for a field change of 7 T, the magnetic entropy change is maximized near phase transition to be 3.05 J kg^{-1} K^{-1} in $Hf_{0.875}Ta_{0.125}Fe_{1.98}$ alloy and 2.95 J kg^{-1} K^{-1} in $Hf_{0.87}Ta_{0.13}Fe_{1.98}$ alloy, which are mainly due to the second-order nature of phase transition. However, once the nature of phase transition is changed to be the weak first-order one, the ΔS^{max} is enhanced to 3.4 J kg^{-1} K^{-1}, which is although lower than 4.8 J kg^{-1} K^{-1} for a field change of 5 T reported in Ref 23.

Since before and after phase transition, the lattice symmetry is unchanged while only the lattice parameter is slightly altered, it means that the thermal expansion ($\Delta L/L$) and magnetostriction (λ) will be abnormal near respective T_c. The temperature-dependent $\Delta L/L$ measured in $Hf_{0.87}Ta_{0.13}Fe_{1.98}$ and $Hf_{0.865}Ta_{0.135}Fe_{1.98}$ alloys along the field directionl under zero field are compared in Fig. 6 with the counterparts measured under 7 T. In $Hf_{0.875}Ta_{0.125}Fe_{1.98}$ alloy, a negative $\Delta L/L$ is observed between 230 K and 273 K. However, under 7 T, the $\Delta L/L$ near T_c is greatly suppressed. Therefore, near T_c, the temperature-dependent saturation magnetostriction ($\lambda^s_{//}$(7 T)) along the direction of external field is also plotted. It is seen that in the ferromagnetic temperature region, with increasing temperature, $\lambda^s_{//}$(7 T) is maximized to be 770 ppm at 273 K and then decreased. Such high $\lambda^s_{//}$(7 T) suggests the sensitive length responses under magnetic field and strong magnetoelastic coupling caused by the phase transition. The linear co-efficiency of negative expansion (α_L) is estimated to be around −17.5 ppm/K between 233 K and 273 K (ΔT = 40 K). On the other hand, in $Hf_{0.865}Ta_{0.135}Fe_{1.98}$ alloy, when temperature is lower than 220 K, the $\Delta L/L$ measured under 0 T is only decreased slowly, leading to the slowly increased $\lambda^s_{//}$(7 T) as the function of temperature. However, when temperature is approaching to T_c, the $\Delta L/L$ measured at zero field decreases fast, leading to a maximized $\lambda^s_{//}$(7 T) of 1800 ppm. However, it is still lower than ~6000 ppm reported in $Hf_{0.83}Ta_{0.17}Ta_{1.98}$ case [10], which is assumed to be originated from different annealing processing. The α_L is increased to −56 ppm/K and compared with those of other systems in table 1. Correlated with the compositional dependence of magnetic entropy change, it is concluded that highest ΔS^{max} is always accompanied with the largest $\lambda^s_{//}$(7 T) of 1800 ppm as observed in $Hf_{0.865}Ta_{0.135}Fe_{1.98}$ alloy, indicating that the largest ΔS^{max} is resulted from the strong magnetoelastic coupling. Noting that Such $\lambda^s_{//}$(7 T) obtained in $Hf_{0.865}Ta_{0.135}Fe_{1.98}$ alloy is also comparable to the saturation magnetostriction of 1600 ~ 1800 ppm of conventional (Tb,Dy)Fe_2 candidate.

To further explore the Ta substitution effects, the magnetic pseudo-binary phase diagram of (Hf, Ta)-Fe is updated as plotted in Fig. 7. The triple critical composition in $Hf_{1-x}Ta_xFe_2$ system is around x = 0.13 and not significantly moved in $Hf_{1-x}Ta_xFe_{1.98}$ system [33–35]. With more Ta substitution, the phase transition from FM to AFM state is decreased faster in the Fe-deficient $Hf_{1-x}Ta_xFe_{1.98}$ system than in $Hf_{1-x}Ta_xFe_2$ system.

4. Conclusions

By Ta substitution, the Tc is monotonously decreased from 303 K to 246 K in $Hf_{1-x}Ta_xFe_{1.98}$ (x = 0.125, 0.13 and 0.135) alloys. The nature of phase transition is also changed from second-order for x = 0.125 to the first-order for x = 0.13 and 0.135, which is evidenced by the thermal and magnetic hysteresis and further by Arrot plots. The magnetic entropy changes measured under 7 T are also enhanced from 3.04 J kg^{-1} K^{-1} to 3.4 J kg^{-1} K^{-1} with widened temperature span with increased Ta content. Such enhanced magnetocaloric effects are strongly correlated with the enhanced magneto-elastic effect, which is further confirmed by the maximized magnetostriction of ~1700 ppm

Table 1
The ΔT and the linear co-efficiency of negative thermal expansion (α_L) of some metallic candidates with negative thermal expansion.

Compounds	ΔT (K)	α_L (ppm/K)
$Hf_{0.863}Ta_{0.135}Fe_{1.98}$ (present work)	220 ~ 259	−56
$Hf_{0.87}Ta_{0.13}Fe_2$ [24]	275 ~ 325	−29.3
$LaFe_{10.5}Co_{1.0}Si_{1.5}$ [27]	240 ~ 350	−26
$Cu_{0.6}Si_{0.15}Ge_{0.25}NMn_3$ [28]	104 ~ 200	−18.4
$Cu_{0.5}Ge_{0.5}NMn_3$ [29]	290 ~ 360	−12.5
$Ga_{0.9}Sn_{0.1}NMn_3$ [30]	279 ~ 338	−27
Epoxy-bonded $MnCoGe_{0.99}In_{0.01}$ [31]	192 ~ 310	−94.7
ZrW_2O_8 [32]	< 425	−9.1
Invar 36 [22]	–	1

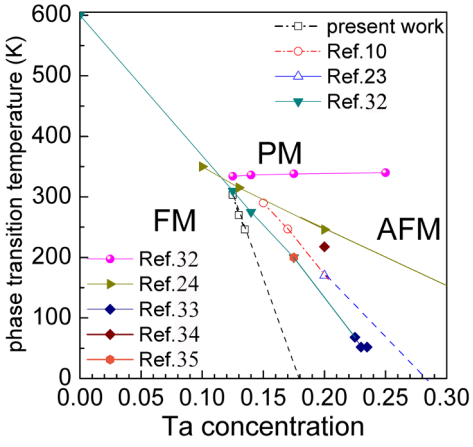

Fig. 7. The updated pseudo-binary phase diagram of (Hf,Ta)-Fe systems. The solid symbols and lines stand for the phase boundary of of (Hf,Ta)Fe_2 system [33–35] while the open symbols and dashed lines for the Fe-deficient (Hf,Ta)$Fe_{1.98}$ system. The pink line and sphere symbols stands for the phase boundary from AFM to PM state. (For interpretation of the references to colour in this figure legend, the reader is referred to the web version of this article.)

near the T_c of $Hf_{0.865}Ta_{0.135}Fe_{1.98}$ alloy.

5. Author statements

All authors are contributing to the work. S. Li performed the experiments of sample preparation and wrote the manuscript. J.C. Yang help the magnetic and magnetostriction measurement. The idea and feasibility of the present work were discussed by X.M. Fan, X.W. Yin, W.B. Cui and Q. Wang. And W.B. Cui and S. Li are responsible for the revised manuscript.

Declaration of Competing Interest

The authors declare that they have no known competing financial interests or personal relationships that could have appeared to influence the work reported in this paper.

Acknowledgements

This work was supported by the major projects of National Natural Science Foundation of China (Grant No. 51690161, 51690162 and 51971056), Fundamental Research Funds for the Central Universities (Grant No. N2009001, N2009002, and N2002005), joint funding between Shenyang National Laboratory for Materials Science and State Key Laboratory of Advanced Processing and Recycling of Nonferrous Metals (Grant No. 18LHPY014), the open fundings of the State Key Laboratory of Solidification Processing in NWPU (Grant No. SKLSP201803) and State Key Laboratory for Mechanical Behavior of Materials (Grant No. 20202206), the Natural Science Foundation of Liaoning Provence (Grant No. 20180510003) and Liaoning Revitalization Talent Program (Grant No. XLYC1907175).

Appendix A. Supplementary data

Supplementary data to this article can be found online at https://doi.org/10.1016/j.jmmm.2020.167236.

References

[1] K. Ikeda, T. Nakamichi, T. Yamada, M. Yamamoto, J. Phys. Soc. Jpn. 36 (1974) 611.
[2] T. Nakamichi, K. Kai, Y. Aoki, K. Ikeda, M. Yamamoto, J. Phys. Soc. Jpn. 29 (1970) 794.
[3] T. Nakamichi, J. Phys. Soc. Jpn. 25 (1968) 1189.
[4] K. Hoshi, J. Phys. Soc. Jpn. 57 (1988) 3112.
[5] Y. Yamada, A. Sakata, J. Phys. Soc. Jpn. 57 (1988) 46.
[6] S. Friedemann, M. Brando, W.J. Duncan, A. Neubauer, C. Pfleiderer, F.M. Grosche, Phys. Rev. B 87 (2013) 024410.
[7] Y. Muraoka, M. Shiga, Y. Nakamura, J. Phys. Soc. Jpn. 40 (1976) 905.
[8] H. Yibole, A.K. Pathak, Y. Mudryk, F. Guillou, N. Zarkevich, S. Gupta, V. Balema, V.K. Pecharsky, Acta Mater. 154 (2018) 365.
[9] H.G.M. Duijn, E. Brück, A.A. Menovsky, K.H.J. Buschow, F.R. de Boer, R. Coehoorn, M. Winkelmann, K. Siemensmeyer, J. Appl. Phys. 81 (1997) 4218.
[10] L. Morellon, P.A. Algarabel, M. Ibarra, Z. Arnold, J. Kamarad, J. Appl. Phys. 80 (1996) 6911.
[11] K. Kai, T. Nakamichi, M. Yamamoto, J. Phys. Soc. Jpn. 29 (1970) 1094.
[12] Y. Nishihara, Y. Yamaguchi, J. Phys. Soc. Jpn. 51 (1982) 1333.
[13] Y. Nishihara, Y. Yamaguchi, J. Phys. Soc. Jpn. 52 (1983) 3630.
[14] Y. Nishihara, Y. Yamaguchi, J. Magn. Magn. Mater. 31–34 (1983) 77.
[15] Y. Nishihara, J. Magn. Magn. Mater. 70 (1987) 75.
[16] C. Zhang, Z. Zhang, S. Wang, H. Li, J. Dong, N. Xing, Y. Guo, W. Li, Solid State Commun. 142 (2007) 477.
[17] C. Zhang, Z. Zhang, S. Wang, H. Li, J. Dong, N. Xing, Y. Guo, W. Li, J. Alloys Compd. 448 (2008) 53.
[18] Y. Nagata, T. Hagii, S. Yashiro, H. Samata, S. Abe, J. Alloys Compd. 292 (1999) 11.
[19] Y.J. Huang, S.J. Li, N. Chen, Y.F. Xia, Nuclear Techniques 30 (2007) 297.
[20] B. Li, X.H. Luo, H. Wang, W.J. Ren, S. Yano, C.W. Wang, J.S. Gardner, K.D. Liss, P. Miao, S.H. Lee, T. Kamiyama, R.Q. Wu, Y. Kawakita, Z.D. Zhang, Phys. Rev. B 93 (2016) 224405.
[21] J.F. Herbst, C.D. Fuerst, R.D. McMichael, J. Appl. Phys. 79 (1996) 5998.
[22] L. Morellon, P.A. Algarabel, M.R. Ibarra, Z. Arnold, J. Kamarád, J. Appl. Phys. 80 (1996) 6911.
[23] J.D. Dong, M.X. Zhang, J. Liu, P.N. Zhang, Aru Yan, Physica B 476 (2015) 171.
[24] L.F. Li, P. Tong, Y.M. Zou, W. Tong, W.B. Jiang, Y. Jiang, X.K. Zhang, J.C. Lin, M. Wang, C. Yang, X.B. Zhu, W.H. Song, Y.P. Sun, Acta Mater. 161 (2018) 258.
[25] Y.Q. Qiao, Y.Z. Song, K. Lin, X.Z. Liu, A. Frans, Y. Ren, J.X. Deng, R.J. Huang, L.F. Li, J. Chen, X.R. Xing, Inorg. Chem. 58 (2019) 5380.
[26] R.J. Huang, Y.Y. Liu, W. Fan, J. Tan, F.R. Xiao, L.H. Qian, L.F. Li, J. Am. Chem. Soc. 135 (2013) 11469.
[27] R.J. Huang, Z.X. Wu, H.H. Yang, Z. Chen, X.X. Chu, L.F. Li, Cryogenics 50 (2010) 750.
[28] Y. Nakamura, K. Takenaka, A. Kishimoto, H. Takagi, J. Am. Ceram. Soc. 92 (2009) 2999.
[29] L.Q. Zhang, D.L. Wang, J. Tan, W. Li, W. Wang, R.J. Huang, L.F. Li, Rare Metal Mater. Eng. 43 (2014) 1304.
[30] Y.Y. Zhao, F.X. Hu, L.F. Bao, J. Wang, H. Wu, Q.Z. Huang, R.R. Wu, Y. Liu, F.R. Shen, H. Kuang, M. Zhang, W.L. Zuo, X.Q. Zheng, J.R. Sun, B.G. Shen, J. Am. Chem. Soc. 137 (2015) 1746.
[31] W. Martienssen, H. Warlimont, Springer Handbook of Condensed Matter and Materials Data (Spinger Berlin Heidelberg New York 2005), p783.
[32] L.V.B. Diop, J. Kastil, O. Isnard, Z. Arnold, J. Kamarad, J. Appl. Phys. 116 (2014) 163907.
[33] R. Rawat, P. Chaddah, P. Bag, P.D. Babu, V. Siruguri, J. Phys.: Condens. Matter 25 (2013) 066011.
[34] P. Bag, R. Rawat, P. Chaddah, P.D. Babu, V. Siruguri, Phys. Rev. B 93 (2016) 014416.
[35] L.V.B. Diop, O. Isnard, E. Suard, D. Bene, Solid State Comm. 229 (2016) 16.